

Interactions between spatial screening solitons propagating in opposite directions

Carmel Rotschild, Oren Cohen, Ofer Manela, Tal Carmon, and Mordechai Segev

Department of Physics and Solid State Institute, Technion, Haifa 32000, Israel

Received January 5, 2004; revised manuscript received March 9, 2004; accepted March 10, 2004

We study experimentally and theoretically collisions between photorefractive spatial solitons propagating in opposite directions and show that each of the interacting solitons significantly affects the self-bending of the other, exhibiting effective attraction for one beam and repulsion for the other. © 2004 Optical Society of America

OCIS codes: 190.4420, 190.5330.

1. INTRODUCTION

Collision between solitons is perhaps the most fascinating feature of soliton phenomena, because the interacting self-trapped wave packets exhibit many particlelike features. Over the years, soliton collisions have been extensively studied theoretically and experimentally, in Kerr and saturable nonlinear media, revealing a variety of effects. Among these are elastic and inelastic collisions, fusion, fission, annihilation, spiraling, and more (for a review see Ref. 1 and references therein). Until recently, all experimental and theoretical work on soliton interactions treated solely solitons propagating in the same general direction, that is, solitons propagating at a small (paraxial) angle with respect to each other. A recent series of papers, however, presented theoretical studies of incoherent²⁻⁴ and coherent^{3,4} interactions between solitons propagating in opposite directions, for the generic Kerr nonlinearity³ as well as for the screening nonlinearity in centrosymmetric² and noncentrosymmetric photorefractive media.⁴ (See Ref. 3 for a detailed explanation of coherent and incoherent interactions between solitons propagating in opposite directions.) Independently of these theoretical studies, Kip's group has performed pioneering collision experiments with solitons propagating in opposite directions in photorefractive waveguides, demonstrating all-optical switching and routing.^{5,6}

In this paper we present an experimental and theoretical study of interactions between one-dimensional photorefractive screening solitons propagating in opposite directions. We have found that the interaction between photorefractive solitons propagating in opposite directions suppresses the self-bending effects of both beams, leading to attraction for one beam and repulsion for the other. We have studied both coherent and incoherent interactions but did not observe differences in the overall interaction effects.

2. THEORETICAL MODEL

We begin by revisiting the theory of one-dimensional photorefractive screening nonlinearity. The space charge field $E_{sc}(x, z)$ satisfies⁷

$$E_{sc} = \frac{E_0}{1 + I} \left(1 + \frac{\epsilon_0 \epsilon_r}{e N_A} \frac{\partial E_{sc}}{\partial x} \right) - \frac{K_b T}{e} \frac{\partial I}{\partial x} \frac{1}{1 + I} + \frac{K_b T}{e} \frac{\epsilon_0 \epsilon_r}{e N_A} \left(\frac{\partial^2 E_{sc}}{\partial x^2} \right), \quad (1)$$

where $I(x, z)$ is the optical intensity (in units of the background illumination), $E_0 = V/L$, V is the voltage applied between electrodes separated by a distance L , k_B is Boltzmann's constant, ϵ_r is the static relative permittivity, N_A is the acceptors density, T is the temperature, e is the electron charge, and x and z are the transverse and the longitudinal propagation directions, respectively. The index change is $\Delta n(I) = (-n_0^3/2)r_{33}E_{sc}$, where n_0 is the unperturbed (linear) refractive index and r_{33} is the relevant term from the electro-optic tensor. Solving Eq. (1) to its lowest-order term results in the usual expression, $E_{sc} = E_0/(1 + I)$, which gives rise to screening solitons.⁸⁻¹² However, the solution to Eq. (1) also includes higher-order terms, including some that are antisymmetric (for $x \rightarrow -x$) for a symmetric beam $I(x) = I(-x)$. These antisymmetric terms are much smaller than the leading term, and hence they do not prohibit soliton formation; they cause an adiabatic tilt in the beam's trajectory toward a preferential crystalline axis. This effect is commonly referred to as the self-bending of photorefractive screening solitons.^{7,10,12} The self-bending effect, although it is evident in all experiments, affects interactions between copropagating screening solitons very little, in both incoherent¹³ and coherent^{14,15} collisions. The reason is straightforward: The trajectories of the interacting solitons, having the same intensity and width, self-bend together, keeping the interaction between them almost unaffected by the bending. Here we show, theoretically and experimentally, that interaction between screening solitons propagating in opposite directions is greatly affected by the self-bending, exhibiting features that are generically different from those of collisions between copropagating screening solitons.

A wave consisting of two beams propagating in opposite directions can be written as³

$$E = F(x, z)\exp[i(kz - \omega t)] + B(x, z) \times \exp[-i(kz + \omega t)] + c.c., \quad (2)$$

where F and B are the forward and backward beams, respectively, normalized to the square root of the background illumination. Here $k = \omega n_0/c$, ω is the temporal frequency, and c is the vacuum speed of light. We are interested here mainly in the incoherent collision scheme,¹³ that is, the situation when the relative phase between F and B varies much faster than the response time of the nonlinear medium, τ . As a result, interference terms such as F^*B average out and do not contribute to the nonlinearity. In such an incoherent collision, space-charge field E_{sc} is a function of the intensity averaged over $t \gg \tau$; thus $\Delta n = \Delta n(\langle I \rangle)$, where $\langle I(x, z) \rangle = |F(x, z)|^2 + |B(x, z)|^2$. Substituting this equation into the nonlinear wave equation, assuming that the nonlinearity is small ($n^2 \cong n_0^2 + 2n_0\Delta n$) and that the solitons are at the same average wavelength, leads to³

$$\frac{\partial^2 F}{\partial x^2} + 2ik \frac{\partial F}{\partial z} = -\frac{2k^2 \Delta n(I)}{n_0} F, \quad (3)$$

$$\frac{\partial^2 B}{\partial x^2} - 2ik \frac{\partial B}{\partial z} = -\frac{2k^2 \Delta n(I)}{n_0} B,$$

where, as noted above, $\Delta n(I) = (-n_0^3/2)r_{33}E_{sc}$ and E_{sc} is given by Eq. (1). We solve Eqs. (3) numerically, using an iterative procedure based on a split-step beam propagation method. We first find the wave functions of screening solitons according to the leading terms^{8,9} (neglecting the self-bending effect) and use them as boundary conditions $F(x, z=0)$ and $B(x, z=L)$. With these, we solve Eqs. (3) iteratively by simulating first the propagation of F in the $+z$ direction (from $z=0$ to $z=L$) and then the propagation of B in the $-z$ direction (from $z=L$ to $z=0$), repeatedly. In every integration step (for each beam separately) we calculate the nonlinearity [by solving Eq. (1)] with the intensity structure of the beam from the previous integration step, and the intensity structure of the oppositely propagating beam as produced in the previous iteration step. We continue until the iterative procedure converges. We verify the accuracy of the solutions by monitoring conserved quantities. We note that this procedure, which was also used in the research reported in Ref. 3, solves for the temporal steady state only and does not describe the temporal evolution as the procedure described in Ref. 4 does. However, when the search is limited to temporal steady-state solutions, the two procedures give the same solutions.

Typical results that display the calculated interaction between solitons incident from the opposite faces of a 5-mm long SBN:60 crystal are shown in Fig. 1. The solitons are 11 μm wide (FWHM) and are launched at almost parallel trajectories, such that the center of the output soliton is displaced by $\sim 29 \mu\text{m}$ from the center of the input soliton at each face of the crystal. In these simulations (as in the experiment) the wavelength is $\lambda = 532 \text{ nm}$, $r_{33} \sim 230 \text{ pm/V}$, $E_0 = 2.8 \text{ [kV/cm]}$, and $F_{\text{max}} = B_{\text{max}} = 6$. The top of Fig. 1 shows the input beams (thick curves) and the output beams (thin solid curves) at

both faces when the solitons are launched simultaneously, i.e., through solution of coupled Eqs. (3) numerically. For comparison, we also calculate the propagation of both solitons when they are launched individually by simulating Eqs. (3) for $B=0$ (dashed curve on face B) and for $F=0$ (dashed curve on face A) separately. To highlight the changes in the self-bending effects, we set the $x=0$ point at the interfaces in Fig. 1 to be at the exit point of the center of each soliton propagating separately. Examining the top of Fig. 1, we find that, on face A, when the solitons are launched simultaneously the bending of the exiting soliton (which is preferentially toward the c axis) is reduced by $\sim 13 \mu\text{m}$ compared with the self-bending of the individually propagating soliton launched from face B and exiting at face A. Likewise, the bending of the soliton exiting at face B (which is also preferentially toward the c axis) is reduced by $2 \mu\text{m}$ compared with the self-bending of the individually propagating soliton launched from face A. The reason for the reduction in self-bending of both exiting solitons can be explained by examination of the middle row in Fig. 1. In both cases, self-bending decreases because the asymmetry of the index profile supporting each exiting self-bending soliton is reduced by the presence of the neighboring soliton propagating in the opposite direction. At face A the reduction in self-bending is dramatic because the (incoherent) attraction between the solitons^{13,16} works together with the reduction in the index asymmetry, the former being a universal property of interacting solitons, whereas the latter is unique to

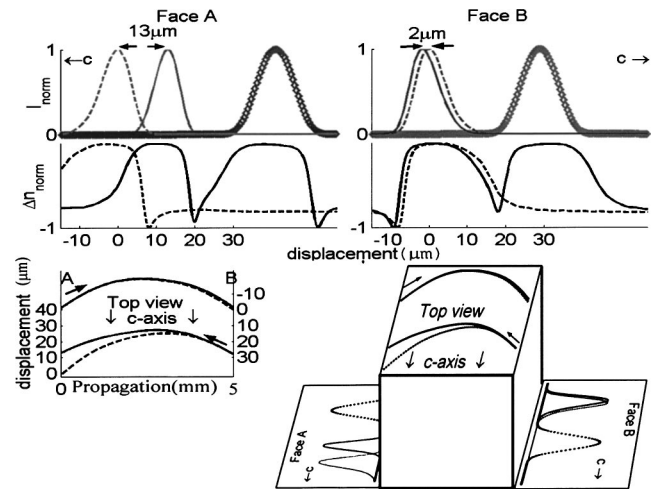


Fig. 1. Calculated interaction between solitons propagating in opposite directions. Top, beam profiles at both faces: input beams (thick curves), output beams when the solitons are launched simultaneously (solid curves), and output beams when the solitons are launched individually (dashed curves). Middle, index change Δn at both faces when the beams are launched simultaneously (thin solid curves) and individually (dashed curves). Bottom left, trajectory of the peak of each soliton when the solitons are launched simultaneously (solid curve) and separately (dashed curve). Bottom right, sketch of the crystal, illustrating a top view of the beam trajectories and beam profiles at both faces. The bending of the exiting soliton at Face A is reduced by $\sim 13 \mu\text{m}$ compared with the self-bending of the individually propagating soliton (this change in bending acts as effective attraction between the solitons). The bending of the soliton exiting at face B is reduced by $\sim 2 \mu\text{m}$ compared with the self-bending of the individually propagating soliton (this change in bending acts as effective repulsion between the solitons).

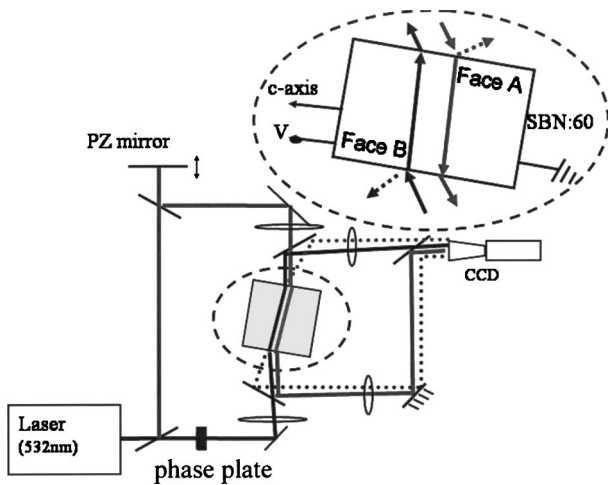


Fig. 2. Experimental setup for studying collisions between solitons propagating in opposite directions.

screening solitons [it arises from Eq. (1)]. At face B, however, the reduction in the index asymmetry has to overcome the incoherent soliton attraction (which here works to increase the self-bending), and thus the reduction in self-bending is smaller. The bottom left-hand part of Fig. 1 shows the trajectory of the peak of each soliton when the solitons are launched simultaneously (thin solid curves) or separately (dashed curves). For clarity, the bottom right-hand part of the figure shows a sketch of the crystal, illustrating a top view of the beam trajectories and beam profiles at both faces.

3. EXPERIMENTAL METHODS

Our experiments are carried out under conditions similar to those of the simulation. The setup (Fig. 2) includes a photorefractive SBN:60 crystal into which two 11- μm FWHM one-dimensional solitons are launched from the opposite faces separated by 5 mm of propagation. The crystal is tilted at an angle of 5° with respect to the normal to the interfaces so as to separate the exiting solitons, the reflections of the input solitons from the crystal faces, and internal reflections. The distance between each input soliton and the output soliton at the same face (when they are simultaneously launched) is 28 μm peak to peak. The applied field is $E_0 = 2.8$ [kV/cm], and the intensity ratio between the peak intensities of the solitons and the background beam is ≈ 36 . To be able to switch between coherent and incoherent interactions, we introduce a piezoelectric (PZ) mirror into one of the optical paths. When the PZ mirror vibrates at 800 Hz the interaction is incoherent, as the nonlinearity cannot follow the interference between the beams. When the mirror is stationary, so is the interference, and the interaction is coherent. The intensity distribution at both faces is monitored by a camera.

4. EXPERIMENTAL RESULTS AND DISCUSSION

Typical experimental results are presented in Fig. 3. First we launch each soliton separately and monitor the exit locations of the solitons at each face (Figs. 3A and

3E), which indicate the bending of the individually launched solitons toward the c axis. Then we launch the solitons simultaneously and let them undergo an incoherent interaction. The soliton exiting at face A bends less by 4.5 μm (Fig. 3B), whereas the soliton exiting at face B bends less by 10 μm (Fig. 3F). We also examine a coherent collision under the same conditions (with the PZ mirror stationary) and observe that the solitons and their bending (Figs. 3C and 3G) are practically identical to those of the incoherent collision. Finally, for comparison, we monitor the linear diffraction (voltage off) of each beam at the output faces. The 11- μm -wide (FWHM) input beams diffract to ~ 36 μm and 40 μm (Figs. 3D and 3H), respectively.

We note that again we do not observe noticeable changes during a coherent collision between the solitons, neither in their widths nor in their trajectories (Figs. 3B, 3F, 3C, and 3G). The coherent effects that occur during the collision arise from interference between the beams, translated into a reflection grating.³ It is therefore essential to ensure experimentally that the coherently interacting solitons maintain mutual coherence at time scales much longer than τ , so the reflection grating is indeed formed. We test for the presence of such a reflection grating at the configuration at which the grating is the strongest, which occurs when the solitons are truly counterpropagating, one on top of the other (together forming a vector soliton as described in Ref. 17). We let the grating form and reach its steady state, and then we block one beam and monitor the reflection of the other beam from the grating as the grating decays in time. This Bragg-matched reflection from the decaying grating is shown in Fig. 4 as a function of time. The existence of this grating proves the occurrence of a stable coherent interaction between the counterpropagating beams. For comparison, when the PZ mirror is vibrating the grating does not form; i.e., the soliton interaction is incoherent, and no reflection is observed from the grating. We therefore con-

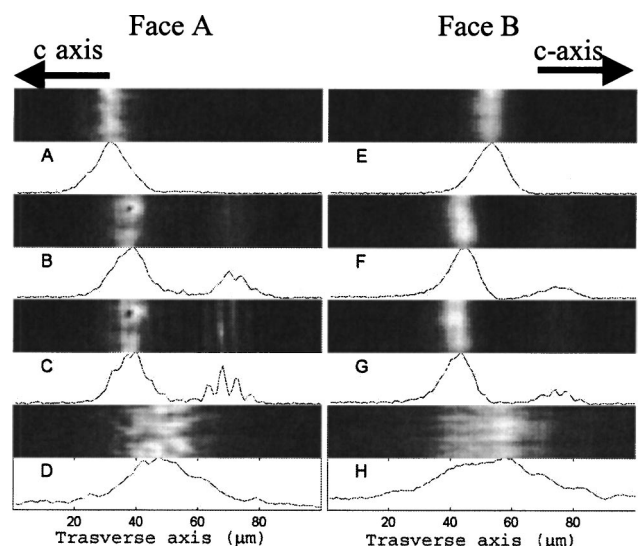


Fig. 3. Experimental results: photographs and intensity profiles of the output beams at both faces for A, E, individually launched solitons; B, F, incoherently interacting solitons; C, G, coherently interacting solitons; and D, H, linearly diffracting beams (at zero voltage).

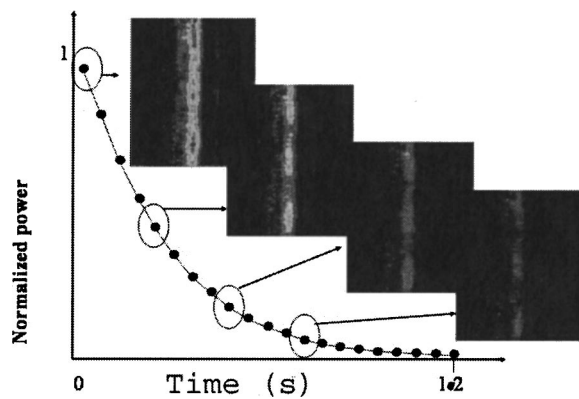


Fig. 4. Decay of the reflection from the grating formed in a vector soliton made from mutually coherent counterpropagating beams, as one beam is blocked (see Ref. 17 for more details).

clude that, experimentally, we do not observe any noticeable difference between coherent and incoherent collisions of photorefractive screening solitons propagating in opposite directions. Evidently, the reflection grating that forms in the coherent interaction between the displaced beams is too weak to affect the interaction significantly. A possible reason could be that the dense periodic modulation (in the z direction) gives rise to strong diffusion effects that limit the strength of E_{sc} in the transverse (x) direction.¹⁸

Before closing, we make a distinction between this work, i.e., studying interactions of solitons propagating in opposite directions, from the related subject of vector solitons formed by counter-propagating beams.^{4,17–21} In the current study, each beam forms a soliton and these solitons interact, whereas, for a vector soliton, each individual constituent does not form a soliton on its own.

5. CONCLUSIONS

To conclude, we have presented an experimental and theoretical study of interactions between photorefractive screening solitons propagating in opposite directions. We have shown that each of the interacting solitons significantly affects the self-bending of the other, exhibiting effective attraction on one side and effective repulsion of the other. The interaction effects in our experiments were dominated by self-bending, whereas the coherent effects that arise from a grating formed between nearly counterpropagating solitons were small. However, the coherent effects that arise during collisions between solitons propagating in opposite directions (predicted in Ref. 3 are generic and interesting; they introduce grating-induced holographic focusing and should lead to a new type of soliton: the holographic soliton.²² Observing holographic solitons is indeed the next experimental challenge.

ACKNOWLEDGMENTS

This work was supported by the German–Israeli DIP Project, the Israeli Science Foundation, and the Israeli Ministry of Science.

REFERENCES AND NOTES

- G. I. Stegeman and M. Segev, "Optical spatial solitons and their interactions: universality and diversity," *Science* **286**, 1518–1523 (1999).
- E. DelRe, A. Ciattoni, B. Crosignani, and P. DiPorto, "Non-linear optical propagation phenomena in near-transition centrosymmetric photorefractive crystals," *J. Nonlinear Opt. Phys. Mater.* **8**, 1–20 (1999).
- O. Cohen, R. Uzdin, T. Carmon, J. W. Fleischer, M. Segev, and S. Odoulov, "Collisions between optical spatial solitons propagating in opposite directions," *Phys. Rev. Lett.* **89**, 133901 (2002).
- M. Belic, Ph. Jander, A. Strinic, A. Desyatnikov, and C. Denz, "Self-trapped bidirectional waveguides in saturable photorefractive medium," *Phys. Rev. E* **68**, 025601 (2003).
- D. Kip, C. Herden, and M. Wesner, "All-optical signal routing using interaction of mutually incoherent spatial solitons," *Ferroelectrics* **135**, 274–278 (2002).
- Similar experiments were carried out in the photorefractive KLTN crystals considered in Ref. 2, but the effects were small because self-bending in such centrosymmetric crystals is tiny (E. DelRe, Universita dell'Aquila, L'Aquila, Italy, personal communication, 2004).
- S. R. Singh, M. I. Carvalho, and D. N. Christodoulides, "Higher-order space charge field effects on the evolution of spatial solitons in biased photorefractive crystals," *Opt. Commun.* **130**, 288–294 (1996).
- M. Segev, G. C. Valley, B. Crosignani, P. DiPorto, and A. Yariv, "Steady-state spatial screening solitons in photorefractive materials with external applied field," *Phys. Rev. Lett.* **73**, 3211–3214 (1994).
- D. N. Christodoulides and M. I. Carvalho, "Bright, dark, and gray spatial soliton states in photorefractive media," *J. Opt. Soc. Am. B* **12**, 1628–1633 (1995).
- M. Shih, M. Segev, G. C. Valley, G. Salamo, B. Crosignani, and P. DiPorto, "Observation of two-dimensional steady-state photorefractive screening solitons," *Electron. Lett.* **31**, 826–827 (1995).
- K. Kos, H. Meng, G. Salamo, M.-F. Shih, M. Segev, and G. C. Valley, "One-dimensional steady-state photorefractive screening solitons," *Phys. Rev. E* **53**, R4330–R4333 (1996).
- M. Shih, P. Leach, M. Segev, M. H. Garrett, G. J. Salamo, and G. C. Valley, "Two-dimensional steady-state photorefractive screening solitons," *Opt. Lett.* **21**, 324–326 (1996).
- M. Shih, Z. Chen, M. Segev, T. Coskun, and D. N. Christodoulides, "Incoherent collisions between one-dimensional steady-state photorefractive screening solitons," *Appl. Phys. Lett.* **69**, 4151–4153 (1996).
- W. Krolikowski and S. A. Holmstrom, "Fusion and birth of spatial solitons upon collision," *Opt. Lett.* **22**, 369–371 (1997).
- H. Meng, G. Salamo, M. Shih, and M. Segev, "Coherent collisions of photorefractive solitons," *Opt. Lett.* **22**, 448–450 (1997).
- D. Anderson and M. Lisak, "Bandwidth limits due to incoherent soliton interaction in optical-fiber communication systems," *Phys. Rev. A* **32**, 2270–2274 (1995).
- O. Cohen, S. Lan, T. Carmon, J. A. Giordmaine, and M. Segev, "Spatial vector solitons consisting of counterpropagating fields," *Opt. Lett.* **27**, 2013–2015 (2002).
- C. Denz, Institute of Applied Physics, Westfälische-Wilhelms-Universität, Münster, Germany (personal communication, 2003).
- M. Haelterman, A. P. Sheppard, and A. W. Snyder, "Bimodal counterpropagating spatial solitary waves," *Opt. Commun.* **10**, 145–152 (1993).
- K. Y. Kolossovski, A. V. Buryak, and R. A. Sammut, "Quadratic solitary waves in a counterpropagating quasi-phase-matched configuration," *Opt. Lett.* **24**, 835–837 (1999).
- K. Motzek, Ph. Jander, A. Desyatnikov, M. Belic, C. Denz, and F. Kaiser, "Dynamic counterpropagating vector solitons in saturable self-focusing media," *Phys. Rev. E* **68**, 06611–06614 (2003).
- O. Cohen, T. Carmon, M. Segev, and S. Odoulov, "Holographic solitons," *Opt. Lett.* **27**, 2031–2033 (2002).